

Evidence of Long Two-Dimensional Folding Chain Structure Formation of Poly(vinylidene fluoride) in *N*-Methylpyrrolidone Solution: Total Form Factor Determination by Combining Multiscattering Data

Erika Saiki, Yuki Nohara, Hiroki Iwase, and Toshiyuki Shikata*



Cite This: *ACS Omega* 2022, 7, 22825–22829



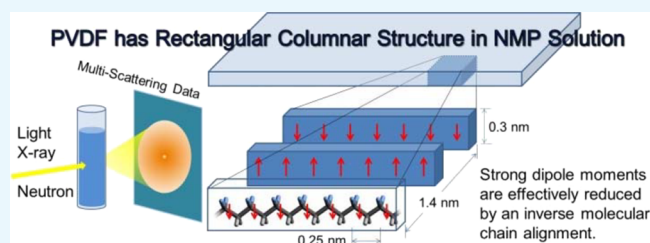
Read Online

ACCESS |

Metrics & More

Article Recommendations

ABSTRACT: Very recently, we proposed that poly(vinylidene fluoride) (PVDF) dissolves in a long rectangular column conformation induced by the formation of a two-dimensional folding chain structure in an *N*-methylpyrrolidone (NMP) solution based on the results obtained from static light scattering (SLS), small- to wide-angle X-ray scattering (S-WAXS), and viscometric experiments. Small- to wide-angle neutron scattering (S-WANS) experiments were able to provide clear decisive evidence for the presence of such a two-dimensional folding chain structure in a deuterated (d)NMP solution of PVDF samples with two different weight average molar masses (M_w) of 100 and 1200 kg mol⁻¹, even under dilute conditions at concentrations less than the overlapping concentrations due to the quite high neutron scattering contrast obtained by using (d)NMP as a solvent. An increase in M_w from 100 to 1200 kg mol⁻¹ substantially increases the particle length and width from $L = 80$ to 350 nm and $w_2 = 5.0$ to 15 nm, respectively, while the thickness, w_1 , is maintained at 0.3 nm. Since L is much longer than w_2 irrespective of M_w , the particles formed by PVDF molecules in NMP simply behave as long rigid rods in a scattering vector (q) range covered by SLS measurements. A combination study of S-WANS and S-WAXS experiments covering a higher q range with the SLS techniques could clearly reveal increases in both the L and w_2 values with increasing M_w .



INTRODUCTION

Very recently, we carried out small- to wide-angle X-ray scattering (S-WAXS) and static light scattering (SLS) experiments in poly(vinylidene fluoride) (PVDF) solutions dissolved in *N*-methylpyrrolidone (NMP) to investigate the conformation and structure of PVDF depending on its weight average molar mass.¹ Although many macromolecular scientists believe that a random coil like conformation of PVDF samples exists in NMP solution as usually observed in other ordinary synthetic polymer solutions, the obtained S-WAXS and SLS data strongly suggested the presence of long rigid rectangular columnar particles formed by the two-dimensional folding chain structure of PVDF molecules.^{1–3} Viscometric measurements also clearly demonstrated rigid rod-like behavior.¹

The observed relationship between the radius of gyration (R_g) and the weight average molar mass (M_w) for each PVDF sample was similar to that of flexible polymer chains in solution, i.e., $R_g \propto M_w^{0.6}$, whereas the form factors resulting from the dependencies of excess Rayleigh ratios (R_θ) on the magnitude of the scattering vectors (q) for PVDF samples in the SLS measurements were reasonably described with rigid rods, i.e., $R_\theta \propto q^{-1}$ in a q range greater than R_g^{-1} , and the

determined particle length (L) demonstrated that the relationship $L^2 \sim 12R_g^2$ held for rigid rods.

S-WAXS experiments, which can provide more local structural information obtained in a q range higher than that of SLS techniques, first showed data suggesting a two-dimensionally developing planar particle structure describable for the observed excess scattering intensities ($\Delta I_X(q)$) in the relationship $\Delta I_X(q) \propto q^{-2}$ in a high q range and rod like behavior, i.e., $\Delta I_X(q) \propto q^{-1}$, in a lower q range with smooth connection to the data observed in the SLS measurements.¹ These observations suggested that PVDF molecules form two-dimensional folding local chain structure resulting in long rectangular columns with thin thicknesses. However, the S-WAXS experiments were carried out under rather low PVDF concentration conditions to prevent molecular chain contacts between PVDF molecules. The obtained $\Delta I_X(q)$ data were

Received: April 20, 2022

Accepted: June 10, 2022

Published: June 21, 2022



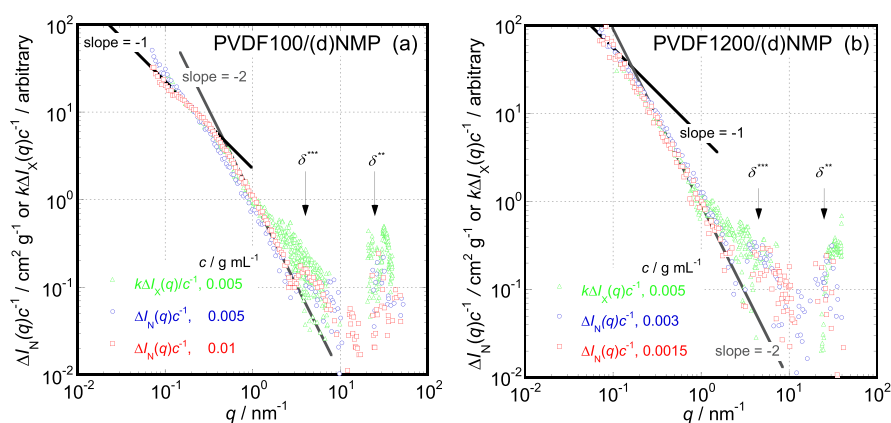


Figure 1. Comparison between $\Delta I_N(q)c^{-1}$ data obtained from S-WANS experiments and $k\Delta I_X(q)c^{-1}$ data obtained from S-WAXS experiments in a previous study¹ for PVDF100 (a) and PVDF1200 (b) solutions dissolved in (d)NMP (S-WANS) and NMP (S-WAXS), respectively. The numerical k values used are identical to each other in both figures.

poorly scattered and the determined local particle size parameters from $\Delta I_X(q)$ data contained uncertainty. In particular, the spacing length existing in the formed two-dimensional folding chain structure estimated from the rather broad shoulder found in the $\Delta I_X(q)$ data of the S-WAXS experiments should be refined using other experimental techniques that possess high sensitivity even at concentrations lower than the overlapping concentrations roughly described by the reciprocal of the intrinsic viscosity ($[\eta]^{-1}$).

It is well known that small- to wide-angle neutron scattering (S-WANS) techniques possess sufficient high sensitivity even under dilute conditions in combined systems between deuterated solutes and usual (protonated) solvents or those between ordinary solutes and deuterated solvents due to high scattering contrasts for neutrons because of a difference in scattering length densities between deuterium and proton atoms.^{4,5} Because fortunately deuterated NMP ((d)NMP) is commercially available, we decided to perform S-WANS measurements in (d)NMP solutions of PVDF samples, which were subjected to S-WAXS experiments in a previous study,¹ to confirm the presence of two-dimensional planar particles formed by the folding chain structure in the (d)NMP solution. The substantial difference in scattering length densities between deuterium atoms in (d)NMP and proton atoms in PVDF would provide more obvious scattering signals due to the spacing present in the formed two-dimensional folding chain structure than the broad shoulder observed in the previous S-WAXS experiments.¹ The overall particle structure formed by PVDF samples in NMP solution can be clarified in more detail by combining the results of SLS, S-WAXS, and viscometric experiments in a previous study and those of S-WANS experiments obtained in this study.

PVDF is one of most important materials to make cathode binder parts contained in many commercial lithium ion secondary batteries, and NMP solutions of PVDF with various M_w values have been practically used in the manufacturing process of cathode binder formation.^{6–8} PVDF has also been used as a useful polymeric material to develop piezoelectric devices due to its unique characteristics such as ferroelectricity, piezoelectricity, and pyroelectricity demonstrated in the solid state effectively caused by the presence of an all-trans zigzag conformation (β -phase or form I) of PVDF chains.^{9,10} Moreover, the content of the β -phase is effectively controllable in the solvent casting process from PVDF

solutions.^{11–14} Therefore, a full understanding of the structure and conformation of PVDF in solution would lead to a breakthrough in processing procedures of new-type lithium ion secondary batteries and mechano-electrical device manufacturing. Then, we complete a detailed discussion of the change in the structure and conformation of PVDF samples dissolved in NMP (and (d)NMP) depending on M_w based on the newly obtained data from S-WANS techniques.

EXPERIMENTAL SECTION

Materials. Two PVDF samples with different M_w values of 100 and 1200 kg mol⁻¹, coded PVDF100 and PVDF1200, were kindly supplied by Kureha Corporation (Tokyo) and used without any further purification processes. Precise molar mass distribution information for these samples is not provided by the company; however, the polydispersity indices (M_w/M_n) are reported to be approximately 2.0. (d)NMP (> 98% in chemical purification and >99% in deuterium enrichment) was purchased from Cambridge Isotope Laboratories, Inc. (Tewksbury) and was used as a solvent to prepare PVDF solutions for S-WANS experiments. The concentrations (c) of PVDF samples were set at 1.0×10^{-2} and 5.0×10^{-3} g mL⁻¹ for PVDF100 and at 3.0×10^{-3} and 1.5×10^{-3} g mL⁻¹ for PVDF1200 samples. To prevent molecular contacts or overlapping in the prepared solutions, such concentrations lower than the reciprocals of intrinsic viscosities ($[\eta]^{-1}$), ca. 1.5×10^{-2} g mL⁻¹ for PVDF100 and ca. 3.4×10^{-3} g mL⁻¹ for PVDF1200,¹ were chosen. Although extrapolation procedures of the concentration, $c \rightarrow 0$, for scattering intensities were necessary to determine form factors of dissolved PVDF molecules precisely, the permitted beam time was strictly limited. Thus, we chose the concentrations to obtain enough scattering intensities to be analyzed without PVDF molecule overlapping.

Methods. S-WANS experiments were performed using a small-angle neutron scattering instrument (TAIKAN)¹⁵ installed in the neutron beamline, BL15, at the Materials and Life Science Experimental Facility (MLF) in Japan Proton Accelerator Research Complex, J-PARC, (Tokai). The covered magnitude range of the scattering vector (q) ranged from 7.0×10^{-2} to 1.0×10^2 nm⁻¹. A banjo-type quartz cell with a neutron path length of 2.0 mm was used as an exposure sample cell. The exposure time of a neutron beam was 2 h for each sample solution and 1 h for the solvent (d)NMP. The

measuring temperature was set at 25 °C for all the S-WANS experiments. The obtained scattering intensities were converted to absolute values using the standard material “glassy carbon”, for which absolute scattering values had been precisely determined.

RESULTS AND DISCUSSION

Comparison between the S-WANS & S-WAXS Data.

Excess neutron scattering intensities ($\Delta I_N(q)$) for each sample solution were evaluated as functions of q via the equation $\Delta I_N(q) = I_N(q) - I_N^{\text{solv}}(q) - I_N^{\text{incoh}}$, where $I_N(q)$, $I_N^{\text{solv}}(q)$, and I_N^{incoh} are the scattering intensity of a tested sample solution, that of the solvent, (d)NMP, and the (small) q independent incoherent component, respectively. The concentration normalized excess scattering intensity, $\Delta I_N(q)c^{-1}$, for each tested sample was used for the consideration of the local structures in the particles formed by the PVDF samples in (d)NMP solution.

The S-WANS experiments performed in this study covered almost the same q range as the S-WAXS experiments in a previous study.¹ Figure 1 shows the comparison between the q dependence profiles of the determined $\Delta I_N(q)c^{-1}$ data and those obtained by S-WAXS experiments, $\Delta I_X(q)c^{-1}$, in a previous study.¹ Although the $\Delta I_N(q)c^{-1}$ data were converted into absolute values, the $\Delta I_X(q)c^{-1}$ data obtained by S-WAXS were not converted. However, the q dependencies can be compared between the two data obtained by different methods for the same PVDF samples. Moreover, because the data were normalized by the concentration, c , the intensities are also comparable with each other. A numerical constant (k) was found, which can reasonably superpose $k\Delta I_X(q)c^{-1}$ on the $\Delta I_N(q)c^{-1}$ data in a q range lower than 1.0 nm⁻¹. Then, Figure 1a was traced out employing the found k value. The same k value used in Figure 1a was also used to make Figure 1b. Because reasonable agreement between the $k\Delta I_X(q)c^{-1}$ and $\Delta I_N(q)c^{-1}$ data is also recognized in the q range less than 1.0 nm⁻¹ in Figure 1b, we might conclude that both the S-WAXS and S-WANS behaviors are essentially identical to each other in the q range not only the dependence on q , but also that on c .

Because the q dependencies of the $\Delta I_N(q)c^{-1}$ (and, of course, $k\Delta I_X(q)c^{-1}$) data for the PVDF100 sample are obviously different from those for the longer PVDF1200 sample, the local structures of the formed particles in these PVDF sample solutions are substantially different from each other, as discussed in a previous study.¹ The q dependence in the PVDF100 system changes from $\Delta I_N(q)c^{-1} \propto q^{-1}$ to $\Delta I_N(q)c^{-1} \propto q^{-2}$ at $q \sim 0.4$ nm⁻¹ as seen in Figure 1a, while the q value where the q exponent alters from -2 to -1 seems to shift to a lower q value close to 0.1 nm⁻¹ in the PVDF1200 system as recognized in Figure 1b.

According to theoretical predictions, the relationship $\Delta I_N(q)c^{-1} \propto q^{-1}$ is the characteristic behavior of a rod-like structure, and $\Delta I_N(q)c^{-1} \propto q^{-2}$ is the characteristic behavior of both random coil and plate-like structures.^{1,16,17} In the case of semiflexible chains such as polymeric samples, the former relationship is always observed in a q range higher than that in which the latter relationship is observed.^{1,18,19} The opposite q range order found in the PVDF systems to the behavior of semiflexible polymer chains strongly suggests that PVDF samples form flat plate particles responsible for the q exponent of -2 in the higher q range, and one side length of the formed plates mainly elongates with increasing M_w values, maintaining its thickness at a constant value similar to long rigid rods,

which show a q exponent of -1 for $\Delta I_N(q)c^{-1}$ in a lower q range. Such a q dependence is well described by the particle form factor ($P(q)$) of a rectangular column with length (L), minor width (w_1) corresponding to the particle thickness, and major width ($w_2 > w_1$), as schematically depicted in Figure 2a.¹

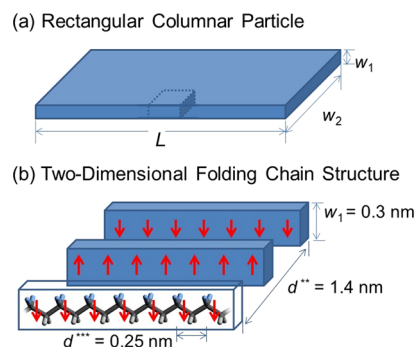


Figure 2. (a) Schematic depiction of a possible particle shape, i.e., a rectangular column with length (L), minor width (w_1) corresponding to the particle thickness, and major width ($w_2 > w_1$), responsible for the q dependence observed in both the S-WANS and S-WAXS experiments. (b) Two-dimensional folding chain structure constructed by the antiparallel alternating arrangement of extended PVDF chain parts in the all-trans conformation in NMP solution. The picture described in panel (b) corresponds to the expansion of a small portion enclosed with dotted lines in panel (a).

The presence of a broad interference peak at $\delta^{***} \approx 4.5$ nm⁻¹ is more clearly observed in the data of the S-WANS experiments than that of the S-WAXS experiments,¹ showing much broader shoulders in a q range from 3 to 5 nm⁻¹ as seen in Figure 1a,b. Although we roughly estimated the spacing distance (d^{***}) corresponding to the small shoulder to be ca. 2.0 nm in the previous study, the clearer peaks observed at ca. 4.5 nm⁻¹ in the $\Delta I_N(q)c^{-1}$ data permit one to determine the spacing to be $d^{***} (= 2\pi/\delta^{***}) \approx 1.4$ nm. Considering the antiparallel alternating arrangement of extended PVDF chain parts in an all-trans conformation in the formed particles in (d)NMP or NMP according to a previous study,¹ the spacing between antiparallel adjacent chains is estimated to be 0.7 nm as schematically depicted in Figure 2b.

An interference peak found at $\delta^{**} \approx 25$ nm⁻¹ in the previous S-WAXS experiments¹ as observed in Figure 1a,b, which corresponds to a spacing distance between adjacent vinylidene groups in the all-trans conformation, i.e., $d^{**} (= 2\pi/\delta^{**}) \approx 0.25$ nm, was not as clearly observed in the S-WANS experiments as in the previous S-WAXS data.¹ Weak excess scattering intensities due to low concentrations to reach the isolated polymer chain condition without contacts between PVDF particles employed in this study are one of the reasons for the difficulty in observing the peak at approximately 25 nm⁻¹. It is possible that this interference peak is essentially more sensitively detectable by X-ray scattering than neutron scattering.

Total Form Factors of PVDF Molecules. The total form factors, $P(q)$, for the tested PVDF molecules are now available, which can describe the q dependencies of the determined excess scattering intensities over the entire q range covered by SLS, S-WANS, and S-WAXS experiments from 7×10^{-2} to 4×10^1 nm⁻¹ and are responsible for the overall structure and conformation of the PVDF molecules. According to the standard SLS theory,^{16,17,20} the intrinsic concentration-reduced

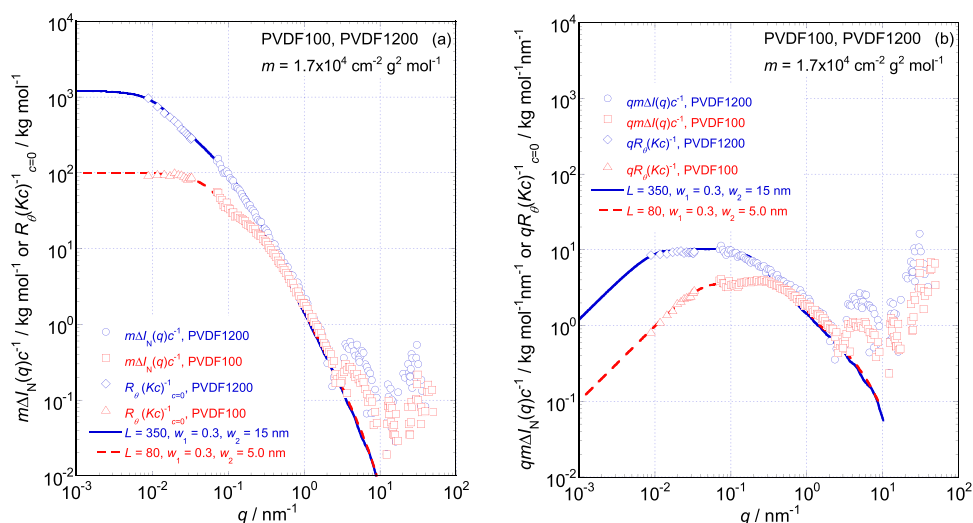


Figure 3. q dependencies of combined $R_{\theta}(Kc)^{-1}_{c=0}$ data previously obtained using SLS techniques¹ and $m\Delta I_N(q)c^{-1}$ data (a) and $qm\Delta I_N(q)c^{-1}$ data (b) for PVDF100 ($c = 0.01$ g mL⁻¹) and PVDF1200 ($c = 0.003$ g mL⁻¹) solutions dissolved in NMP (SLS) and (d)NMP (S-WANS). The same constant value of $m = 1.7 \times 10^4$ cm⁻² g² mol⁻¹ was used to produce the combined data. The solid and broken lines represent the q dependencies of the total form factors, $P(q)$, of rectangular columns²¹ proposed for particles formed by PVDF samples with different M_w values examined in this study. The size parameters, L , w_1 , and w_2 used to calculate $P(q)$ are listed in the figure.

excess Rayleigh ratios determined at $c = 0$ g mL⁻¹ using the extrapolation procedures, $R_{\theta}(Kc)^{-1}_{c=0}$, where K is an apparatus-dependent constant, are identical to $M_w P(q)$. On the other hand, a proportional constant connecting the c independent $\Delta I_N(q)c^{-1}$ value as obtained in this study with $P(q)$, such as M_w in the SLS theory, exists and must be proportional to M_w .^{4,5,16,17} Then, the relationship $R_{\theta}(Kc)^{-1}_{c=0} = m\Delta I_N(q)c^{-1}$ holds with a certain proportional constant m , which is independent of M_w and can be determined under various experimental conditions.

Using the constant value of $m = 1.7 \times 10^4$ cm⁻² g² mol⁻¹, the $\Delta I_N(q)c^{-1}$ data of PVDF100 ($c = 0.01$ g mL⁻¹) and PVDF1200 ($c = 0.003$ g mL⁻¹) were combined to the $R_{\theta}(Kc)^{-1}_{c=0}$ data obtained using SLS techniques in a previous study¹ and shown in Figure 3a. The solid and broken lines seen in Figure 3a represent $M_w P(q)$ curves for the PVDF samples determined previously assuming rectangular columns possessing $L = 80$, $w_2 = 5.0$, and $w_1 = 0.3$ nm for PVDF100 and $L = 350$, $w_2 = 15.0$, and $w_1 = 0.3$ nm for PVDF1200.¹ The q dependencies of these form factors, $P(q)$, for rectangular column particles²¹ were precisely calculated via multipurpose open source software SasView,²² which is useful for various kinds of scattering data analyses.¹ The $m\Delta I_N(q)c^{-1}$ data of both PVDF samples are smoothly linked to the $R_{\theta}(Kc)^{-1}_{c=0}$ data, and the $M_w P(q)$ lines reproduce the q dependencies of both the $R_{\theta}(Kc)^{-1}_{c=0}$ and $m\Delta I_N(q)c^{-1}$ data over almost the entire q range examined except for the interference signals observed at ca. 4.5 nm⁻¹ as seen in Figure 3a. These observations strongly suggest that the assumed rectangular columnar form factors, $P(q)$, obtained by combining scattering data obtained by using the S-WANS, S-WAXS, and SLS techniques, reasonably satisfy the essential characteristics of the particles formed by the PVDF samples with different M_w values and reasonably behave as the total form factors.

Figure 3b shows the q dependencies of $qR_{\theta}(Kc)^{-1}_{c=0}$ and $qm\Delta I_N(q)c^{-1}$ data, so called the Holzer plot,²³ for the PVDF solutions shown in Figure 3a. If the formed particles have the rigid rod structures, $qR_{\theta}(Kc)^{-1}_{c=0}$ and $qm\Delta I_N(q)c^{-1}$ data clearly show plateaus in the q range of $R_g^{-1} < q < R_c^{-1}$, where

R_c is the cross-sectional radius of the formed rods. The height of the observed plateau theoretically means $\pi M_w/L$ corresponding to the weight average mass per unit length of the rods.²³ The plateau values observed in Figure 3b, 3.8 and 10 kg mol⁻¹ nm⁻¹, respectively, in a q range of $R_g < q < (0.5w_1)^{-1}$ (instead of R_c^{-1} for rigid rods) reasonably agree with the $\pi M_w/L$ values, 3.9 and 11 kg mol⁻¹ nm⁻¹, for each PVDF sample. Because the formed rectangular columnar particles of PVDF samples in NMP solutions have an L much longer than the width w_1 , such an argument based on the rigid rod particle structure seems to hold approximately.

The highly elongated rectangular columnar particle structure resulting from the determined form factor provides the M_w dependence of the intrinsic viscosity, $[\eta]$, calculated via a widely accepted theoretical model for rigid rods^{24,25} suspended in a liquid medium, which reasonably agrees with experimental results.¹ This strongly supports the validity of the form factor determined through combining multidata obtained from the S-WANS, S-WAXS, and SLS techniques in this study.

CONCLUSIONS

Combining the data obtained by small- to wide-angle neutron scattering, S-WANS, small- to wide-angle X-ray scattering, S-WAXS, and static light scattering, SLS, experiments realized the total form factor determination for poly(vinylidene fluoride), PVDF, samples dissolved in *N*-methylpyrrolidone, NMP (and (d)NMP), which can reasonably describe the structure and conformation of particles formed by PVDF molecules in the solution. PVDF molecules form elongated rectangular columnar-shape particles in NMP solution. The elongated PVDF molecules approximately in the all-trans conformation are sequentially arrayed in the antiparallel manner of electric dipole moments due to the presence of fluoride atoms in the NMP solution. The two-dimensional folding structure formed by a PVDF chain resembles a long rectangular column possessing length L , major width w_2 ($\ll L$), and minor width (thickness) w_1 ($< w_2$). The values of L and w_2 increase with increasing M_w , while w_1 remains at a constant value of approximately 0.3 nm irrespective of M_w .

AUTHOR INFORMATION

Corresponding Author

Toshiyuki Shikata – Division of Natural Resources and Eco-materials, Graduate School of Agriculture and Cellulose Research Unit, Tokyo University of Agriculture and Technology, Fuchu 183-8509, Japan; orcid.org/0000-0001-6846-4985; Email: shikata@cc.tuat.ac.jp

Authors

Erika Saiki – Division of Natural Resources and Eco-materials, Graduate School of Agriculture and Cellulose Research Unit, Tokyo University of Agriculture and Technology, Fuchu 183-8509, Japan

Yuki Nohara – Cellulose Research Unit, Tokyo University of Agriculture and Technology, Fuchu 183-8509, Japan

Hiroki Iwase – Neutron Science and Technology Center, Comprehensive Research Organization for Science and Society (CROSS), Tokai, Ibaraki 319-1106, Japan; orcid.org/0000-0003-4038-7839

Complete contact information is available at:

<https://pubs.acs.org/10.1021/acsomega.2c02483>

Funding

Japan Proton Accelerator Research Complex, J-PARC.

Notes

The authors declare no competing financial interest.

ACKNOWLEDGMENTS

This study was partially supported by Japan Proton Accelerator Research Complex, J-PARC, (Tokai). Small- to wide-angle neutron scattering experiments were performed at the Materials and Life Science Experimental Facility of the J-PARC under a user program (Proposal No. 2021I0015). The authors thank Misaki Ueda (CROSS) for her support on the S-WANS measurements. All the poly(vinylidene fluoride) samples were kindly supplied by Kureha Corporation (Tokyo).

REFERENCES

- (1) Nohara, Y.; Saiki, E.; Shikata, T. Long Two-Dimensional Folding Chain Structure Formation of Poly(vinylidene fluoride) in Solutions of a Polar Solvent, N-Methylpyrrolidone. *ACS Appl. Polym. Mater.* **2022**, *4*, 1255–1263.
- (2) Welch, G. J. Solution properties and unperturbed dimensions of poly(vinylidene fluoride). *Polymer* **1974**, *15*, 429–432.
- (3) Luttringer, G.; Weill, G. Solution properties of poly(vinylidene fluoride): 1. Macromolecular characterization of soluble sample. *Polymer* **1991**, *32*, 877–883.
- (4) Maconnachie, A.; Richards, R. W. Neutron scattering and amorphous polymers. *Polymer* **1978**, *19*, 739–762.
- (5) Feigin, L. A.; Svergun, D. I.; Taylor, G. W. *Principles of the Theory of X-Ray and Neutron Scattering*; Springer: Boston, 1987; Chapters 1 and 6.
- (6) Chen, H.; Ling, M.; Hencz, L.; Ling, H. Y.; Li, G.; Lin, Z.; Liu, G.; Zhang, S. Exploring chemical, mechanical, and electrical functionalities of binders for advanced energy-storage devices. *Chem. Rev.* **2018**, *118*, 8936–8982.
- (7) Zhang, X.; Ross, P. N., Jr.; Kostecki, R.; Kong, F.; Sloop, S.; Kerr, J. B.; Striebel, K.; Cairns, E. J.; McLarnon, F. Diagnostic Characterization of High Power Lithium-Ion Batteries for Use in Hybrid Electric Vehicles. *J. Electrochem. Soc.* **2001**, *148*, A463–A470.
- (8) Buqa, H.; Holzapfel, M.; Krumeich, F.; Veitc, C.; Novák, P. Study of styrene butadiene rubber and sodium methyl cellulose as binder for negative electrodes in lithium-ion batteries. *J. Power Sources* **2006**, *161*, 617–622.
- (9) Fukada, E. History and Recent Progress in Piezoelectric Polymers. *IEEE Trans. Ultrason. Ferroelectr. Freq. Control* **2000**, *47*, 1277–1290.
- (10) Poulsen, M.; Ducharme, S. Why Ferroelectric Polyvinylidene Fluoride is Special. *IEEE Trans. Dielectr. Electr. Insul.* **2010**, *17*, 1028–1035.
- (11) Hasegawa, R.; Kobayashi, M.; Tadokoro, H. Molecular conformation and packing of poly(vinylidene fluoride). Stability of three crystalline forms and the effect of high pressure. *Polym. J.* **1972**, *3*, 591–599.
- (12) Hasegawa, R.; Takahashi, Y.; Chatani, Y.; Tadokoro, H. Crystal structures of three crystalline forms of poly(vinylidene fluoride). *Polym. J.* **1972**, *3*, 600–610.
- (13) Gregorio, R., Jr.; Ueno, M. E. Effect of crystalline phase, orientation and temperature on the dielectric properties of poly(vinylidene fluoride) (PVDF). *J. Mater. Sci.* **1999**, *34*, 4489–4500.
- (14) Nishiyama, T.; Takayuki, S.; Eriko, S.; Horibe, H. Effect of solvents on the crystal formation of poly(vinylidene fluoride) film prepared by a spin-coating process. *Polym. J.* **2017**, *49*, 319–325.
- (15) Takata, S.; Suzuki, J.; Shinohara, T.; Oku, T.; Tominaga, T.; Ohishi, K.; Iwase, H.; Nakatani, T.; Inamura, Y.; Ito, T.; Suzuki, K.; Aizawa, K.; Arai, M.; Otomo, T.; Sugiyama, M. The Design and q Resolution of the Small and Wide Angle Neutron Scattering Instrument (TAIKAN) in J-PARC. *JPS Conf. Proc.* **2015**, *8*, 036020.
- (16) Pedersen, J. S. Analysis of small-angle scattering data from colloids and polymer solutions: modeling and least-squares fitting. *Adv. Colloid Interface Sci.* **1997**, *70*, 171–210.
- (17) Glatter, O. *Scattering Methods and their Application in Colloid and Interface Science*; Elsevier: Amsterdam, 2018; Chapters 9 & 10.
- (18) Yoshizaki, T.; Yamakawa, H. Scattering Functions of Wormlike and Helical Wormlike Chains. *Macromolecules* **1980**, *13*, 1518–1525.
- (19) Pedersen, J. S.; Schurtenberger, P. Scattering functions of semiflexible polymers with and without excluded volume effects. *Macromolecules* **1996**, *29*, 7602–7612.
- (20) Debye, P. Molecular-weight determination by light scattering. *J. Phys. Colloid Chem.* **1947**, *51*, 18–32.
- (21) Nayuk, R.; Huber, K. Formfactors of Hollow and Massive Rectangular Parallelepipeds at Variable Degree of Anisometry. *Z. Phys. Chem.* **2012**, *226*, 837–854.
- (22) SasView, <https://www.sasview.org/>; Doucet, M. et al. SasView Version 5.0.3, Zenodo, DOI: 10.5281/zenodo.3930098; access data was September, 10th, 2021.
- (23) Holtzer, A. Interpretation of the angular distribution of the light scattered by a polydisperse system of rods. *J. Polym. Sci.* **1955**, *17*, 432–434.
- (24) Ortega, A.; García de la Torre, J. Hydrodynamic properties of rodlike and disklike particles in dilute solution. *J. Chem. Phys.* **2003**, *119*, 9914–9919.
- (25) Doi, M.; Edwards, S. F.; *The Theory of Polymer Dynamics*. Clarendon Press: Oxford, 1986; Chapter 8.